Crimson Publishers
Wings to the Research

Research Article

Recycling of Glass Waste in Ceramics-Part II: Microstructure of Ceramic Products using XRD, DTA and SEM Techniques

Darweesh HHM*

Refractories, Ceramics and Building Materials Department, National Research Centre, Egypt

ISSN: 2576-8840

***Corresponding author:** Darweesh HHM, Refractories, Ceramics and Building Materials Department, National Research Centre, Egypt

Submission: May 18, 2020

Published: May 27, 2020

Volume 13 - Issue 4

How to cite this article: Darweesh HHM. Recycling of Glass Waste in Ceramics-Part II: Microstructure of Ceramic Products using XRD, DTA and SEM Techniques. Res Dev Material Sci. 13(4). RDMS.000817. 2020. DOI: 10.31031/RDMS.2020.13.000817

Copyright@ Darweesh HHM, This article is distributed under the terms of the Creative Commons Attribution 4.0 International License, which permits unrestricted use and redistribution provided that the original author and source are credited.

Abstract

The current study is to follow the previous published paper about the physical, mechanical and thermal characteristics of traditional ceramic composites incorporating different ratios of glass waste. The phase composition and/or microstructure of the optimum ceramic batch (G5) compared with those of the blank (G0) was investigated by X-ray Diffraction Patterns (XRD), Differential Thermal Analysis (DTA) and Scanning Electron Microscopy (SEM). The XRD analysis proved that the resulting ceramic product exhibited higher strength than that of the blank due to the formation of new ceramic phases which were responsible for the higher values of densification parameters as well as mechanical strength. The DTA thermo grams illustrated the dissociation and conversion of the various phases. The SEM micrographs showed that the well crystallized and well developed crystals of G5 offered the excellent external apprearrans and/or microstructure of the samples incorporated glass waste.

Keywords: Glass waste; Ceramic products; Microstructure; XRD; DTA; SEM

Introduction

Scope of the problem

It is well known that nanotechnology differs from a field to a field and from a place to a place and it is essentially used to describe very small things [1-3]. Nanotechnology is to make materials less than 100nm, i.e. nanomaterials to convert it into materials with essentially new and fine features and functions [4,5]. The overwhelming demand and interest of nanotechnology is so one of the most exciting disciplines that it almost interferes into all applied science branches as: physics, chemistry, materials sciences, biology, agriculture, medicine, tissue engineering, bones caffolds, dentistery, ceramics, nanoceramics, bio ceramics and in a general biomaterials because the nanoparticles are highly efficient additives for the modification of ceramic products, even at small ratios (1-2wt. %). The author interests with using nanomaterials or accurately nanoparticles to prepare ceramic batches containing ultra fine and nano raw materials as nano-SiO_2 and nano-Al_2O_3 to indicate the importance of nano particles, to improve the physical, chemical, mechanical properties and thermal properties as: thermal shock, thermal expansion, firing resistance, and also durability of the resulting bio products against aggressive environments. Recently, nanomaterials are the basis and backbone of nanotechnology. Nanomaterials are of a great interest due to the fact that unique optical, rheological and electromagnetic properties could be arised. These features are of a great importance in nanomaterials-based on nanoceramics [6,7]. Scientists have not unanimously settled on a precise definition of nanomaterials, but agree that they are partially characterized by their size that measured in nanometers. A nanometer is one millionth of a millimeter- approximately 100,000 times smaller than the diameter of a human hair. Nanomaterials by definition must have at least one dimension that is less than approximately 100 nanometers. Most nanoscale materials are too small to be seen with the naked eye, and even with conventional lab microscopes. Nanomaterials can be added to huge number of materials to make them stronger and yet lighter. Nanomaterials have very small size particles which are having 1-3 dimensions ≤100nm or may be more, i.e. Nanomaterials can be created with various dimensions.

In recent years, nanomaterials have taken an over welming interest due to that nano ceramics are flexible at high firing temperatures if compared with those containing coarse size particles [1,7-13]. The increase in the various solid waste residues in the cities particularly those do not decompose easily neither in nature, nor by weathering factors for thousands of years such as wastes of glass bottle that created the growth of both ground and air populations. The recycling of these wastes is an important environmental and economical alternative solution [14-22].

In Egypt, there are huge quantities of waste glass bottles of several shapes, colors and sizes. This certainly causes an environmental problem like as the ground pollution. Therefore, it is very necessary to solve this serious problem through scientific researches that could use these priceless waste materials in traditional ceramics like as wall and/or floor tiles, table wares or porcelain stoneware tiles. These may be used for out and/or indoor applications. Thus, the glass waste can act as inert component in total replacement of quartz sand, and also can act as fluxing agent at the expense of feldspar totally. Clay is a product which is coming from the decomposition of granite rocks that is represented of about 75% of the earth's crust, and it is essentially composed of alumina (Al_2O_3) and silica (SiO_2), i.e. these two minerals are of the major constituents of clay [23,24].

Objectives of the study

The main objective of the present study (Part II) is to analyze and detect the new formed phases and microstructure of the prepared traditional ceramic products made from clay, feldspar, limestone and quartz in combination with glass waste nanoparticles using XRD, DTA and SEM techniques, where In Part I [25], the physical, thermal and mechanical properties were investigated.

Experimental

Raw materials

The clay sample (TC) was taken from Toshka region which is located on latitude 20º 30′ N and longitude 31º 53′ E at 250km south of Aswan. It was related to the Upper Cretaceous age. The selected clay deposit is belonging to El- Dakhla Shale Formation. About 10kg clay was collected from the 85thkm north of Aswan/ Abu-Semple asphaltic road. It is a dark yellowish grey. The clay sample was first well dried in an open air for three days and also in a suitable furnace at 105 **ºC** for another three days, then crushed, ground and quartered to have a representative sample which was fine ground to pass a 200 mesh sieve using a suitable agate mortar. Feldspar (F), quartz (Q) from El-Hekma firm, limestone (LS) from Samalout district and a waste of broken fired ceramic known as Grog (GG) were obtained from the Arab Ceramic Company, which is commercially known as Aracemco, Egypt. Also, the glass waste bottles do decompose easily neither in nature, nor by weathering factors (Figure 1). The chemical analysis using the X-ray fluorescence technique (XRF) and the particle size distribution of the starting raw materials are shown in Table 1 & 2, respectively.

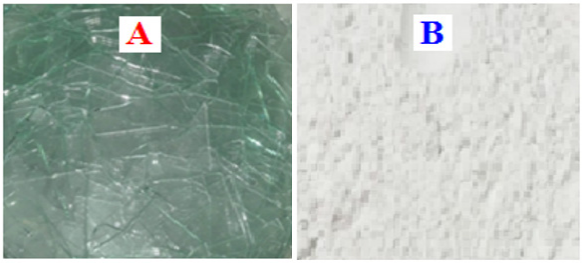

Figure 1: Glass waste cullet (A) and glass waste powder (B).

Table 1: Chemical analysis of the starting raw materials.

Oxides	Raw Materials					
	TC	F	Q	LS	GG	G.W
SiO_2	51.47	75.37	93.63	0.08	61.73	70.31
Al_2O_3	28.78	13.62	3.64	0.02	28.11	2.46
Fe_2O_3	3.99	0.41	0.08	0.3	7.50	0.26
CaO	0.61	0.53	0.18	56.83	0.91	8.69
MgO	1.38	---	---	0.11	0.37	3.62
MnO	0.04	0.03	0,02	---	-----	0.02
Na_2O	1.15	3.44	0.17	0.13	1.24	13.52
K_2O	1.19	5.84	0.14	0.06	1.39	1.06
SO_3	--	0.02	0.14	0.02	---	---
TiO_2	1.14	0.05	0.16	0.01	1.57	0.12
P_2O_5	0.53	---	---	---	-----	0.02
Cl	--	0.02	0.06	0.08	----	---
Cr_2O_3	--	---	---	---	----	0.01
LOI	9.72	0.67	1.78	42.63	---	---
Total	100	100	100	100	100	100

Copyright © Darweesh HHM

Table 2: The grain size distribution of the used raw materials, wt. %.

Particle Size, %	Raw Materials				
	TC	F	Q	LS	GW
> 63	1.43	0.17	0.13	0.13	0.19
- 63-16	1.68	0.13	0.15	0.18	0.28
- 16-8	2.96	0.89	0.12	0.18	0.12
- 8-2	9.14	10.43	4.58	1.17	6.46
< 2	84.79	88.38	95.12	98.34	92.95
Total, wt.%	100	100	100	100	100

Preparation and Methods

The suggested base ceramic batch was prepared from 50% Clay (TC), 20% feldspar (F), 15% quartz (Q), 10% limestone (LS) and 5% grog (GG). The base batch composition was well mixed in an agate ball mill for one hour using the wet method. Then, it lets to dry in open air for two days and also in a dryer at 105 ºC for three days. Thoroughly, it crushed and ground well to pass through 200 mesh sieve to be the stock base ceramic tile batch. Eight batches were prepared from the base batch (BB) and glass waste (GW) as 100:0, 95:5, 90:10, 85:15, 80:20, 75:25, 70:30 and 65:35 mass% having the symbols G0, G1, G2, G3, G4, G5, G6 and G7, respectively. The batches were mixed well in agate ball mill using 3-5 porcelain balls for two hours, dried again at 105 **ºC** for three days, and then let to pass through a 200 mesh sieve to obtain the same homogeneity of all batches. Five disc-shaped samples of 1cm diameter and 1cm thickness were prepared for the physical properties in terms of water absorption (WA), bulk density (BD) and apparent porosity (AP). Another five rod-shaped samples of $1\times1\times7cm^3$ for dry and firing shrinkage, thermal expansion and bending or flexural strength were prepared. Also, five cylindrical shaped samples of one cm diameter and 3cm height for crushing strength were prepared. The molding of specimens were carried out under a shaping pressure of $20KN/mm^2$ using water as a binder. After remolding, the samples were let to dry in air (23**±**2 **ºC**) for 2-3 days, and then dried to a constant weight at 105 **ºC** in a suitable oven to ensure the complete elimination of the free water and to avoid the cracks during firing. The fired specimens were left to cool slowly over night inside the furnace to room temperature. The optimum firing temperature and the optimum GW content of each ceramic batch were estimated. The tested specimens of the base batch (G0) and those containing glass waste (G1-G7) were subjected to follow up the firing shrinkage for each batch [25].

In the Part II, we will follow the phase compositions and/or the microcrystalline structure of the optimum ceramic batch which achieved the best results (G5) in comparison with the blank (G0) were investigated by X-ray Diffraction Analysis (XRD), Differential Thermal Analysis (DTA) and Scanning Electron Microscopy (SEM) techniques to identify the newly formed crystalline materials or phases after sintering process. The X-ray Diffraction Analysis (XRD) was employed by a Philips X-Ray Diffractometer of Mod. P.W. 1390 with Ni-filtered Cu-K**α** radiation. The DTA-TGA thermo grams was carried out by using NETZSCH Geratebae GmbH Selb, Bestell No. 348472c at a heating rate 10 **ºC**/min. up to 1200 **ºC**. The SEM micrographs were done by using JEOL-JXA-840 electron analyzer at accelerating voltage of 30KV. The fractured surfaces were fixed on Cu-k**α** stubs by carbon paste and then were coated with a thin layer of gold.

Results and Discussion

In Part I [25], the physical characteristics in terms of densification parameters as water absorption, bulk density, apparent porosity as well as mechanical properties in terms of flexural and crushing strengths were investigated. Moreover, the thermal behavior of the resulting ceramic products in terms of dry and firing shrinkage, thermal expansion also was conducted. In addition, the coefficient of linear thermal expansion was further investigated. The use glass waste nano particles with an original ceramic batch to produce wall and floor tiles, where eight different mixtures with various ratios of glass waste nano particles were prepared (0, 5, 10, 15, 20, 25, 30 and 35% having the symbols G0, G1, G2, G3, G4, G5, G6 and G7), respectively, and then fired in a temperature range of 1000-1200 **ºC** for two hours soaking. Results showed that the water absorption decreased as the glass content increased up to 35% if fired up to 1100 **ºC**. On firing >1100 **ºC**, the water absorption decreased only up to 25% glass content (G5), and then increased with G6 and G7. The bulk density of all batches increased up to 1100 **ºC**. On firing >1100 **ºC**, the bulk density increased only up to 25% glass waste content, and then decreased with further increase of glass waste content. The mechanical properties in terms of flexural and crushing strengths were displayed the same trend of bulk density. The dry shrinkage recorded zero reading, i.e. it was unchanged, while the firing shrinkage was slightly increased with both glass content and firing temperature. The experimental results revealed that the glass contributes to improve thermal, physical and mechanical properties as well as microstructure of the prepared samples containing up to 25 wt. % of glass waste fired at 1150 **ºC**. The addition of high amounts of glass waste (>25 wt. %) into the ceramic body is undesirable due to its adverse action on physical and mechanical properties of the fired products. Moreover, the external appearance of the ceramic units was too bad, i.e. surface bloating. The dry shrinkage was unchanged, but the firing shrinkage was increased with both temperature and glass waste content. The coefficient of linear thermal expansion decreased with glass waste content.

In Part II, the microstructure of the produced optimum ceramic unit using XRD, DTA and SEM techniques were evaluated in comparing with those of the blank. Table 1 shows the composition analysis of the starting raw material, while Table 2 showed the grain size distribution of glass waste. It is clear that there are high ratios of SiO_2, CaO, MgO and Na_2O and detectable low ratios of TiO_2, Fe_2O_3, SO_3, Al_2O_3, K_2O, MnO, Cl^- and K_2O were observed in the raw materials. Also, a detectable Na_2O ratio was noted in the glass waste composition. These ratios besides the grain size distribution could be helped in the sintering of the ceramic units during firing.

Copyright © Darweesh HHM

Characterization of clay and glass waste

Figure 2 demonstrates the DTA-TGA thermo grams of clay sample (TC). The endothermic peak at the temperature range of 700-900 **ºC** is due to the calcination of limestone. The two endothermic peaks at the temperature range 100-120 **ºC** and 500-600 **ºC** are due to the evaporation of the absorbed and structural or hygroscopic water, respectively. The endothermic peak at the temperature range 500-600 **ºC** is due to the conversion of kaolinite (Al_2O_3.2 SiO_2.2H_2O) to metakaolin (Al_2O_3.2SiO_2), which in turn is converted to mullite phase ($3Al_2O_3$.2SiO_2) at 980 **ºC [25]**. The XRD analysis of the used clay and glass waste samples are shown in Figure 3. Clay is essentially composed of kaoline, quartz, illite and gibbsite, whereas that of the waste glass is composed mainly of quartz and minor traces of other oxides [25].

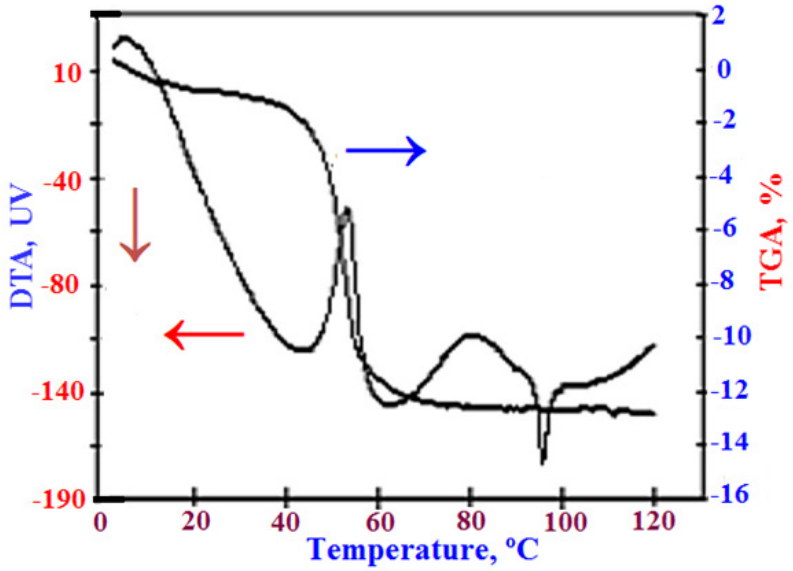

Figure 2: The DTA-TGA thermo grams of the used clay sample.

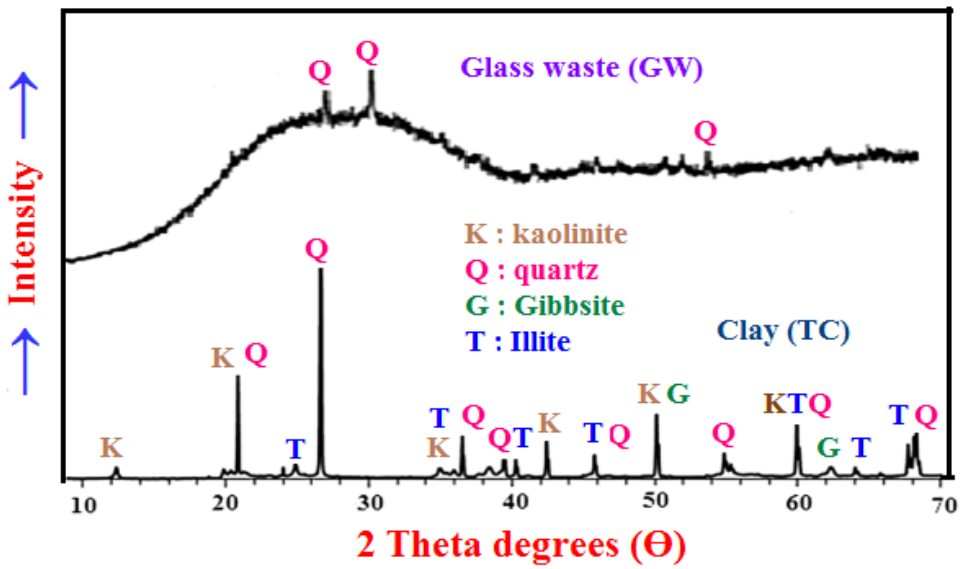

Figure 3: The XRD patterns of the Toshka clay sample and waste glass powder.

X-ray Diffraction Patterns (XRD)

The XRD diffraction patterns of the well sintered blank sample (G0) and the optimum ceramic product (G5) are shown in Figure 4. It is clear that quartz, walstromite ($BaCa_2Si_3O_9$, ICCD no 18-0162) and also wollastonite ($CaSiO_3$, ICCD 84-0654) are detected in case of the blank sample, whilst in case of the optimum sample (G5), the well crystallized and well developed phases of wollastonite, spurrite, anorthite and mullite phases were developed. The resulting new well sintering phases during firing and sintering are responsible for the better characteristics of the physical, mechanical and thermal properties of the formed ceramic products [10,25-29].

Copyright © Darweesh HHM

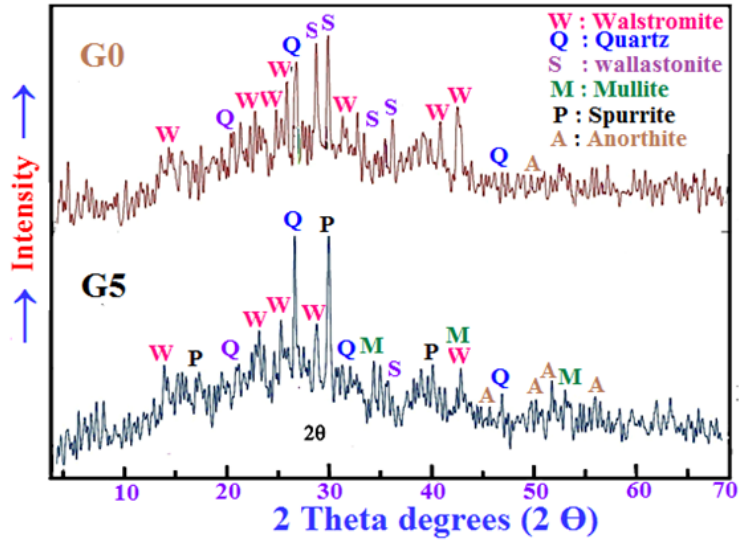

Figure 4: The X ray diffraction patterns of the sintered 3 and 4 samples.

Differential Thermal Analysis (DTA)

The phase transformations of the blank batch (G0) and the optimum batch (G5) were estimated by DTA thermo grams as shown in Figure 5. The endothermic peak at the temperature range of 450-680 **ºC** is due to the evaporation of the free or absorbed water and/or the hygroscopic or structural water. Also, the endothermic peak at the temperature range of 860-960 **ºC** is attributed to the dehydroxylation and the conversion kaolinite ($Al_2O_3.2SiO_2.2H_2O$) into metakaolin ($Al_2O_3.2SiO_2$) as shown in the equation 1. It is also due to the calcination of limestone. The endothermic peak at the temperature range of 1100-1850 **ºC** is mainly due to the melting of feldspar and may be also silica quartz [30,31]. Moreover, it is due to the crystallization of the glass frits incorporated in the different batches.

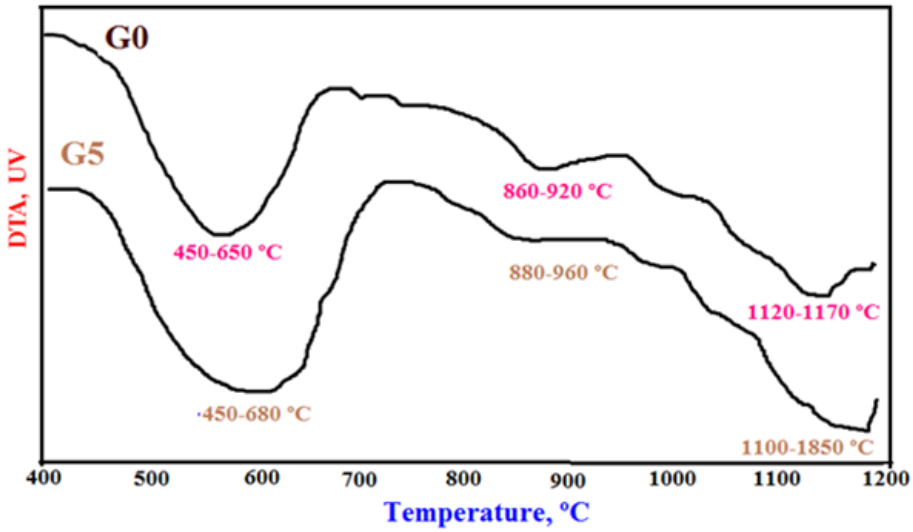

Figure 5: The DTA thermograms of the well sintered samples G0 and G5 at 1000 °C.

Scanning Electron Microscopy (SEM)

The SEM microscopy of the well sintered sample at 1000 **ºC** of the optimum sample G5 comparing with that of the blank (G0) is shown in Figure 6. This was carried out with two magnification powers. The image of the blank sample (G0) shows large rounded pores with the embedded lathes and rods around the glassy groundmass. A similar texture was developed with the optimum sample (G5), but with more well developed and well crystallized sheet or cluster structures, but with little pores. There are several particulates with various shapes and sizes as flocculants or almost globulars. The formed new phases seemed to be as thick fibers which supported the resulting ceramic products. This is responsible for the improvement of the physical and mechanical properties. Moreover, this improved the external appearance of the formed ceramic units, and so enhanced the mechanical strength of them [9,10,27-29,32].

Copyright © Darweesh HHM

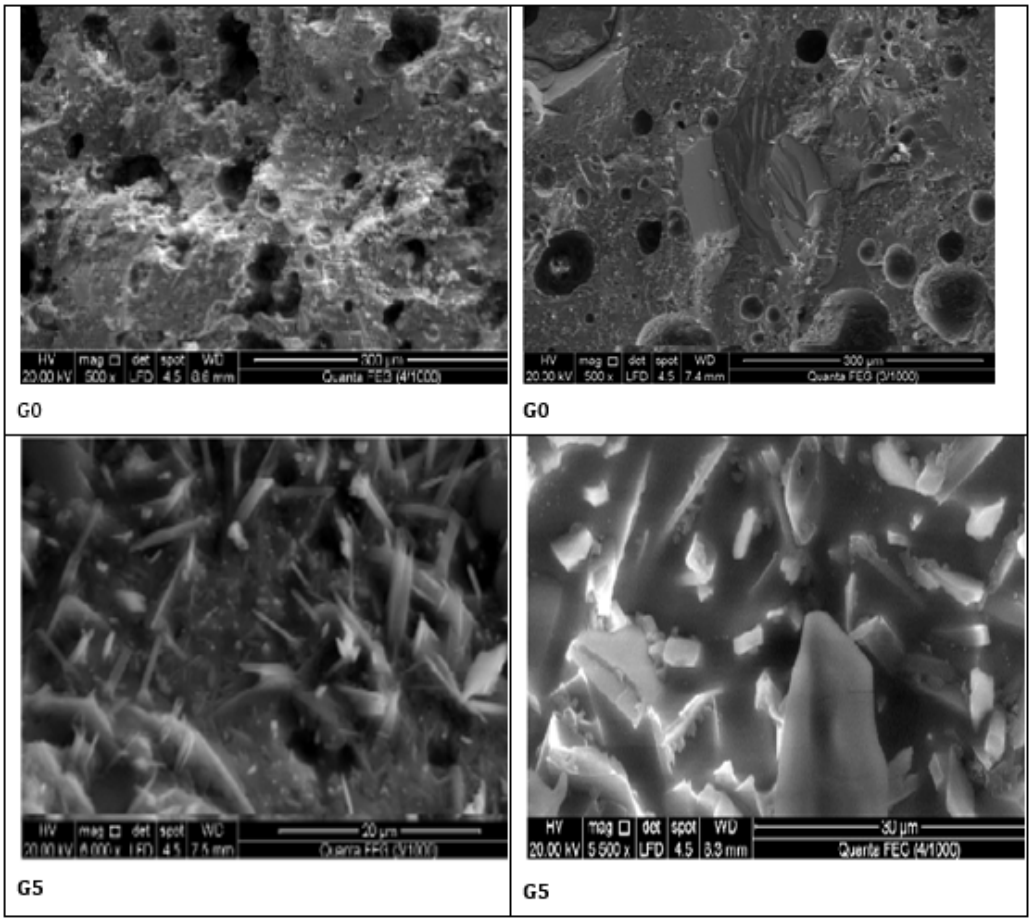

Figure 6: SEM micrographs of the well sintered samples G0 and G5 at 1000 °C.

General Discussion

There are two successive processes namely, sintering and verification. The reactions could be taken place between constituents on heating as solid phase reactions which are the first step towards densification, even when it is followed by the formation of liquid phase or not at all. This process is a mutual diffusion of atoms among the touching particles, which is known as "sintering". As a result, the particles become fewer and larger, and then the pores are eliminated or reduced. The verification (i.e. glass formation) may start to form in the ceramic bodies above 900-1000 **ºC** depending on the composition of these bodies. The particles of feldspar which used as a flux and glass waste which used as a secondary or modifying flux could react with the constituents of other ingredients which they are in contact to form the liquid phase. The quantity of this liquid phase increases with the increase of firing temperature. Often, the fired ceramic bodies contract during firing due to the formation of the liquid phase which is known as "firing shrinkage". So, the porosity of the bodies as well as water absorption reduced, while the bulk density increased [28,33].

New phases may be crystallized, particularly as the temperature increased as mullite ($3Al_2O_3.2SiO_2$) which usually separated from the melt. On cooling, more other crystals may be separated and the liquid itself solidifies to a glass after cementing the unmelted particles together. This often finished by the formation of a glass matrix with crystal aggregates. The presence of MgO, CaO, K_2O and Na_2O is the main reason controlling the maturing temperature, liquid phase formation, crystallization of the new phases and the resulting densification properties. The MgO in glass waste favors the conversion of quartz to **α**-tridymite and then to **α**-cristobalite [34-36].

The presence of alkali oxides (Na_2O and K_2O) from feldspar and/or glass waste enhanced the liquid phase content, and lowered the viscosity at higher firing temperatures to improve the verification process. The formed liquid phase always favors the conversion reaction of quartz to **α**-cristobalite rather than the dissolution of MgO into it. However, the quantity of SiO_2 dissolved in the glassy matrix only has a small effect on the amount and composition of the liquid phase [33]. The major influence of alkalies is to alter the relative amounts of **α**-cristobalite and liquid phase up to the maturing temperature. Furthermore, the temperature dependence of the verification rate of a certain composition as that used in the current study is greater than that of viscosity alone. This is to be expected in the presence of glass waste due to the increased liquid phase content at the firing temperatures to reach the suitable maturing conditions. Also, the addition of CaO, as that existed in the glass waste in forms of carbonates, sulphates or silicates, the formation of gehlenite ($2CaO.Al_2O_3.SiO_2$), wollastonite (**β**-$CaO.SiO_2$), anorthite $CaO.Al_2O_3.2SiO_2$), spurrite ($2C_2S.CaCO_3$) as well as C_3A was

Copyright © Darweesh HHM

enhanced. So, the crystallization of these solid phases was increased which in turn improves and enhances the densification properties of the ceramic body containing glass waste [31]. This is due to the enhancement of verification and sintering processes together to reach the best conditions that governs the function of the liquid phase to close the pores as well as its role to conduct bonding of solid phases present together resulting in higher densities [28,35-37].

Generally, clay minerals are often formed from the decomposition of igneous rocks as granite which is composed mainly of roughly equal proportions of potash mica ($K_2O.3Al_2O_3.6SiO_2.2H_2O$), quartz ($SiO_2$) and potash feldspar ($K_2O.Al_2O_3.6SiO_2$). The kaolinitic clay was due to the kaolinization of feldspar in presence of air and water [16,25,28] as follows:

$$K_2O.3\ Al_2O_3.6\ SiO_2 + H_2O \rightarrow Al_2O_3.2\ SiO_2.2H_2O + K_2O + 4SiO_2 \quad \text{-----1}$$

The most important clay minerals is kaolinite ($Al_2O_3.2SiO_2.2H_2O$ or AS_2H_2), which appears as flat and extremely minute hexagonal plates. The crystal size may vary from 5**μ** to 1**μ** (or 10-4 meters), which in turn is responsible for their extreme properties [28-31] as the plasticity or workability which simplifies the manufacture of clay wares and also account for the dry strength of the unfired article. So, this helps to reduce handling losses. At the temperature range 100-200 **ºC**, the volume of certain argillaceous minerals shrinks as a result of water loss causing a dimensional change. The oxidation of organic materials occurs at the temperature range 200-300 **ºC** [32-35]. Kaolinite which is a decomposition product of feldspar, often decomposes at 500-600 **ºC** to metakaolin ($Al_2O_3.2SiO_2$ or AS_2) and water vapor [25,28,31] as follows:

$$Al_2O_3.2SiO_2.2H_2O \rightarrow Al_2O_3.2SiO_2 + 2H_2O \text{ -------- 2}$$

This reaction was often accompanied by an expansion, i.e. the ceramic units enlarged. At about 980 **ºC**, a sudden evolution of heat accompanies the complete breakdown of the structure with the formation of mullite ($3Al_2O_3.2SiO_2$) and quartz minerals as follows:

$$Al_2O_3.2SiO_2 \rightarrow 3Al_2O_3.2SiO_2 + SiO_2 \text{ ----- 3}$$

The transformation of quartz into cristobalite is slow and it depends on the firing temperature and time of firing. At 573 **ºC**, **β**-quartz converts into **α**-quartz, which converted into **α**-tridymite at 870 **ºC**, which in turn converted to **α**-cristobalite at 110-1470 **ºC**, as follows:

β-quartz → **α**-quartz ------ 4

α-quartz → **α**-tridymite ----- 5

α-tridymite → **α**-cristobalite -------- 6

There are two types of feldspar namely orthoclase potash feldspar ($K_2O.Al_2O_3.6SiO_2$) and albite soda feldspar ($Na_2O.Al_2O_3.6SiO_2$), in addition to small ratios of mica and silica. Feldspar starts to melt at high temperature depending on the total alkali content and particle size distribution of materials. Limestone is an important ingredient in tiles due to its ability to reduce moisture expansion [33,34]. Limestone is often used at about 10-12wt. % in tile bodies to reduce the amount of glassy phase during firing. At 700-900 **°C**, it decomposes to CaO and CO_2 as follows:

$$CaCO_3 \rightarrow CaO+CO_2\uparrow \text{-------7}$$

Then, the resulting CaO can react with other constituents to form anorthite-lime feldspar ($CaAl_2Si_2O_8$) rather than enter into the glassy phase. The reduction in glass content virtually eliminates firing shrinkage [33].

Conclusion

It is well known now that the thermal reactions during firing and sintering plays a vital role to evaluate the mechanisms of thermal behavior, and to separate the reactivates of single components especially with respect to multi component systems. This in turn could be an advantage, and this will be the ultimate challenge for the next years. We are looking forward to a bright future for the use of glass wastes in useful application. It could be concluded that the XRD patterns, DTA thermo grams and SEM microscopy of the selected samples of the blank (G0) and the optimum sample (G5) proved that some new well crystallized and well developed phases were detected with G5 incorporated glass waste when compared with those of the blank (G0). The DTA analysis showed the decomposition and transformation of different minerals during firing and sintering. These new formed phases were responsible for the excellent results previously obtained with glass waste. This study could be applied successfully in both pilot scale and/or industry. The SEM images showed clearly that with G5 sample, there are well developed morphological and crystal phases when compared with those of the blank sample (G0).

Acknowledgement

Authors wish to express their deep thanks to NRC for helping to obtain materials, processing, preparing, molding and measuring all of the obtained data of the study.

References

1. (2000) Nalwa HS (Ed.), Handbook of Nanostructured Materials and Nanotechnology, Academic Press, San Diego, CA, USA.
2. (2004) Nalwa HS (Ed.), Encyclopedia of Nanoscience and Nanotechnology, American Scientific Publishers, Los Angeles, CA, USA.
3. Shackelford JF (2004) Introduction to materials science for engineers. (6th edn), Prentice Hall, USA.
4. Darweesh HHM, Kenawy SH (2020) Light-weight highly porous building bricks from Sawdust. Indian Journal of Engineering 17: 193-2030.
5. Poole CPJr, Owens FJ (2003) Introduction to nano technology, Wiley-Interscience.
6. Darweesh HHM (2018) Nanomaterials: classification and properties-Part I. J Nanosci 1(1): 1–11.
7. Darweesh HHM (2018) Nanoceramics: materials, properties, methods and applications-Part II. J Nanosci 1(1): 40-66.
8. Rawlings RD, Wu JP, Boccaccini AR (2006) Glass-ceramics: Their production from wastes - a review. Journal of Materials Science 41: 733-761.
9. Ashby MF, Shercliff HR, Cebon D (2007) Materials: Engineering, science, processing and design, Butterworth Heinemann, UK.

Copyright © Darweesh HHM

10. Ashby MF, Ferreira PJ, Schodek DL (2009) Nanomaterials, nanotechnology and Design. Text Book, Elsevier Ltd,.

11. Sobolev K, Ferrada-Gutiérrez M (2005) How nanotechnology can change the concrete, world: Part 1. Am Ceram Soc Bull 84(10): 14-17.

12. Tseng TY, Nalwa HS (2009) Handbook of Nanoceramics and Their Based Nanodevices, American Scientific Publishers, Los Angeles, CA, USA.

13. Callister WD (2007) Materials Science and Engineering. An introduction, (7th edn), Wiley.

14. Tucci A, Esposito L, Rastelli E, Palmonari C, Rambaldi E (2004) Use of soda lime scrap-glass as a fluxing agent in a porcelain stoneware tile mix. J Eur Ceram Soc 24: 83-92.

15. Lin KL (2007) Use of thin film transistor liquid crystal display (TFT-LCD) waste glass in the production of ceramic tiles. J Hazard Mater 148: 91-97.

16. Vieira CMF, Monteiro SN (2009) Incorporation of solid wastes in red ceramics-an updated review. Rev Matér 14: 881-905.

17. Hojamberdiev M, Eminov A, Xu Y (2011) Utilization of muscovite granite waste in the manufacture of ceramic tiles. Ceram Int 37: 871-876.

18. Nuttawat K, Jaimasith M, Thiemsorn W (2013) Fabrication of ceramic floor tiles from industrial wastes. Suranaree J Sci Technol 21:6 5-77.

19. Furlanin E, Maschio S (2013) Mechanical properties and microstructure of fast fired tiles made with blends of kaolin and olivine powders. Ceram Int 39(8): 9391-9396.

20. Kim K, Hwang J (2016) Characterization of ceramic tiles containing LCD waste glass. Ceram Int 42: 7626-7631.

21. Ke S, Wang Y, Pan Z, Ning C, Zheng S (2016) Recycling of polished tile waste as a main raw material in porcelain tiles. J Clean Prod 115: 238-244.

22. Amin SK, Sibak HA, El-Sherbiny SA, Abadir MF (2016) An overview of ceramic wastes management in construction. Int J Appl.

23. Sahar MR, Hamzah K, Rohani MS (2011) The micro structural study of cullet-clay ceramics. Phys Procedia 22: 125-129.

24. Kourti I, Cheeseman CR (2010) Properties and microstructure of lightweight aggregate produced from lignite coal fly ash and recycled glass. Resour Conserv Recycl 54: 769-775.

25. Darweesh, HHM (2019) Recycling of glass waste in ceramics-part I: physical, mechanical and thermal properties. SN Applied Sciences 1: 1274.

26. Abadir MF, Sallam EH, Bakr IM (2002) Preparation of porcelain tiles from Egyptian raw materials. Ceramics International 28: 303-310.

27. Raimondo M, Zanelli C, Matteucci F, Guarini G, Dondi M, et al. (2007) Effect of waste glass (TV/PC cathodic tube and screen) on technological properties and sintering behaviour of porcelain stoneware tiles. Ceramics International 33: 615-621.

28. Darweesh HHM, Wahsh MMS, Negim EM (2012) Densification and thermo mechanical properties of conventional ceramic composites containing two different industrial byproducts, Amer. Eurasian Journal of Scientific Research 7(3): 123-130.

29. Darweesh HHM (2015) Ceramic wall and floor tiles containing local waste of cement kiln dust- Part I: Physical properties. American Journal of Civil Engineering and Architecture 2: 35-43.

30. Karamanov A, Karamanova E, Ferrari AM, Ferrante F, Pelino M (2006) The effect of scrap addition on the sintering behavior of hard porcelain. Ceramics International 32: 727-732.

31. Zanelli C, Baldi G, Dondi M, Ercolani G, Guarini G, et al. (2008) Glass ceramic frits for porcelain stoneware bodies: effects on sintering, phase composition and technological properties. Ceramics International 34: 455-465.

32. Darweesh HHM (2016) Ceramic wall and floor tiles containing local waste of cement kiln dust- Part II: Dry and firing shrinkage as well as mechanical properties. American Journal of Civil Engineering and Architecture 4(2): 44-49.

33. Chiang YM, Birnie DP, Kingery WG (1997) Physical ceramics-principals for ceramic science and engineering. (3rd edn), John Wiley and Sons, Lehigh Press. Inc., USA.

34. Bragança SR, Licenzi J, Guerino K, Bergmann CP (2006) Recycling of iron foundry sand and glass waste as raw material for production of white ware. Waste Management & Research 24: 60-66.

35. Souza AJ, Pinheiro BCA, Holanda JNF (2010) Recycling of gneiss rock waste in the manufacture of vitrified floor tiles. Environm Management J 91(3): 685-689.

36. Souza AJ, Pinheiro BCA, Holanda JNF (2010) Processing of floor tiles bearing ornamental rock-cutting waste. Materials Processing Technology 210(14): 1898-1904.

37. Darweesh HHM, Awad HM, Tawfik A (2011) Red bricks from dakhla formation clay-Tushka area-Incorporated with some Ind. Wastes or byproducts, Industrial Ceramics 31(3): 201-207.

For possible submissions Click below:

Submit Article

Copyright © Darweesh HHM